



ACADEMIC
PRESS

Available online at www.sciencedirect.com

SCIENCE @ DIRECT®

Journal of Solid State Chemistry 173 (2003) 387–394

JOURNAL OF
SOLID STATE
CHEMISTRY

<http://elsevier.com/locate/jssc>

Crystal structure and thermal behavior of a new cadmium indium oxalate

Erwann Jeanneau, Nathalie Audebrand, and Daniel Louër*

Laboratoire de Chimie du Solide et Inorganique Moléculaire (UMR 6511 CNRS), Institut de Chimie, Université de Rennes, Avenue du Général Leclerc, 35042 Rennes Cedex, France

Received 4 December 2002; received in revised form 17 February 2003; accepted 20 February 2003

Abstract

A new mixed metal oxalate $\text{Cd}_3\text{In}_2(\text{C}_2\text{O}_4)_6 \cdot 9\text{H}_2\text{O}$, with an open-framework structure, has been prepared from a precipitation method at room temperature. Its crystal structure has been solved from single-crystal diffraction data. The compound crystallizes with space group $P6_422$ and the cell parameters are $a = 8.566(5) \text{ \AA}$, $c = 37.811(5) \text{ \AA}$, $V = 2403(2) \text{ \AA}^3$, and $Z = 3$ ($R_1 = 0.036$). The three-dimensional structure is built from three types of MO_8 ($M = \text{Cd}, \text{In}$) polyhedra, i.e., triangular dodecahedra, bicapped trigonal prisms and an undefined distorted eight-fold cadmium polyhedron. Relationships with the structures of the related cadmium zirconium oxalates are discussed. The structure overview suggests the possibility to conceive new oxalate-based materials with open-framework structures. The thermal behavior of the new compound is described in details from temperature-dependent X-ray powder diffraction and thermogravimetry measurements. The dehydration process of the precursor is reversible in its stability temperature range. The final product consists of a mixture of nanocrystalline CdIn_2O_4 and the simple oxides.

© 2003 Elsevier Science (USA). All rights reserved.

Keywords: Cadmium indium oxalate; Single-crystal diffraction; Crystal structure; Open-framework; Porous materials; Eight-fold polyhedral coordination; Thermal decomposition; Temperature-dependent powder diffraction; Mixed cadmium indium oxide

1. Introduction

The synthesis of new compounds with open-framework structures has received considerable attention over the last few years (see, for example, Refs. [1–3]). Indeed, their topology could make these compounds eligible for interesting applications in catalysis, ionic exchanges or sorption processes. In recent years, our activity has focused on the elaboration of new open-framework architectures based on the assembly of polyhedra formed by eight-fold coordinated metals and linked together through oxalate ligands (Refs. [4,5] and references therein). The careful analysis of the reported structures reveals that the structural topologies of all phases are based on the assembly of either triangular dodecahedra or square-based antiprisms polyhedra [4–8], which are the most frequently encountered geometries for eight-coordinate complexes [9–11]. A

representative example is the Cd/Zr/oxalate system, in which two distinct open-framework topologies, having the same chemical composition, $[\text{CdZr}(\text{C}_2\text{O}_4)_4]^{2-}$, have been reported (see Fig. 7 in Ref. [4]). The additional cations are localized in the channels of the structures together with weakly bonded water molecules, which confer to the material specific zeolitic properties [6,7]. Since a similar framework was also found in the Y/K/oxalate system, in which both cations are eight-fold coordinated, the extension to other eight-fold coordinated metals, such as indium, has been considered. Indeed, eight-fold coordinated In atoms have been reported in the structure of a mixed indium ammonium oxalate [12], as well as in the structure of $\text{In}_2(\text{C}_2\text{O}_4)_3 \cdot 10\text{H}_2\text{O}$ [13]. The present study deals with the synthesis, the crystal structure and the thermal behavior of a new mixed metal oxalate, $\text{Cd}_3\text{In}_2(\text{C}_2\text{O}_4)_6 \cdot 9\text{H}_2\text{O}$. Additionally, the crystal structure is compared to those of related oxalate-based phases and the In and Cd environments are discussed in terms of polyhedral shapes found for eight-fold complexes.

*Corresponding author. Fax: +33-2-99-38-34-87.

E-mail address: daniel.louer@univ-rennes1.fr (D. Louër).

2. Experimental

2.1. Preparation and preliminary characterization

Crystals of cadmium indium oxalate $\text{Cd}_3\text{In}_2(\text{C}_2\text{O}_4)_6 \cdot 9\text{H}_2\text{O}$ were obtained from a mild chemistry route. The compound was synthesized from a mixture of 0.50 g of cadmium nitrate $\text{Cd}(\text{NO}_3)_2 \cdot 4\text{H}_2\text{O}$ from Merck and 0.6 g of anhydrous indium chloride InCl_3 from Alfa Aesar, dissolved in 50 mL of deionized water. This solution was titrated by a 0.1 mol L^{-1} oxalic acid solution in excess until a white precipitate was formed. The mixture was heated up to 60°C under stirring and $\sim 15 \text{ mL}$ of concentrated HNO_3 was slowly added until complete dissolution of the precipitate. After two days, the evaporation of the solution at room temperature led to the formation of thick, transparent hexagonal-plated crystals of average size $50 \mu\text{m}$. The crystals were then filtered, thoroughly washed with deionized water and ethanol, and finally dried in air. The X-ray diffraction pattern of the powdered crystals indicated that the product was a new material. It was subsequently verified that the powder pattern fitted well the simulated one generated from the single-crystal structure solution reported in the present study, which demonstrates the purity of the material. The chemical formula was derived from Energy Dispersive X-ray Spectrometry (ratio $\text{Cd}/\text{In} = 3/2$), performed by means of a JSM 6400 spectrometer equipped with an Oxford Link Isis analyzer, and from the crystal structure determination reported below. It is in agreement with the chemical composition $\text{Cd}_3\text{In}_2(\text{C}_2\text{O}_4)_6 \cdot 9\text{H}_2\text{O}$. Assuming the above formula, the yield found for this synthesis was 86% based on cadmium.

2.2. X-ray diffraction data collection

A suitable crystal was mounted on a four-circle Nonius Kappa CCD diffractometer, using $\text{MoK}\alpha$ radiation ($\lambda = 0.71073 \text{ \AA}$) and equipped with a CCD area detector. Intensities were collected by means of the program COLLECT [14]. Reflection indexing, Lorentz-polarization correction, peak integration and background determination were carried out with the program DENZO [15]. Frame scaling and unit-cell parameters refinement were achieved with the program SCALEPACK [15]. A numerical correction absorption was performed by modeling the crystal faces using NUMABS [16]. The resulting set of hkl reflections was used for structure refinement. Crystallographic data and details on data collection are listed in Table 1. Structure drawings were carried out with Diamond 2.1e, supplied by Crystal Impact [17].

X-ray powder diffraction data were obtained with a Siemens D500 diffractometer with the para-focusing Bragg–Brentano geometry, using monochromatic

Table 1

Crystallographic data and structure refinement parameters for $\text{Cd}_3\text{In}_2(\text{C}_2\text{O}_4)_6 \cdot 9.03\text{H}_2\text{O}$

Empirical formula	$\text{Cd}_3\text{In}_2\text{C}_{12}\text{O}_{33.03}\text{H}_{18.06}$
Crystal system	Hexagonal
Space group	$P6_422$ (No. 181)
Crystal size (mm)	$0.025 \times 0.045 \times 0.050$
a (Å)	8.566(5)
c (Å)	37.811(5)
Volume (Å ³)	2403(2)
Z	3
Formula weight (g mol ⁻¹)	1260.72
ρ_{calc} (g cm ⁻³)	2.616
λ (MoK α) Å	0.71073
θ range (deg)	1.62–30.03
Index ranges	$-12 \leq h \leq 12$, $-12 \leq k \leq 12$, $-53 \leq l \leq 53$
Observed data ($I > 2\sigma(I)$)	2339
R_1 ($I > 2\sigma(I)$)	0.036
R_1 (All)	0.048
wR_2 ($I > 2\sigma(I)$)	0.091
wR_2 (All)	0.097
Refinement method	Full-matrix least-squares on $ F^2 $
Goodness of fit	1.097
No. of variables	123
Largest difference map peak and hole (e Å ⁻³)	2.138 and -1.089

$\text{CuK}\alpha_1$ radiation ($\lambda = 1.5406 \text{ \AA}$) selected with an incident beam curved-crystal germanium monochromator [18].

2.3. Thermal analysis

Thermogravimetry analyses (TG) were carried out with a Rigaku thermoflex instrument for runs under airflow. The powdered samples were spread evenly in large platinum crucibles to avoid mass effects. Temperature-dependent X-ray diffraction (TDXD) was performed under dynamic air with a powder diffractometer combining the curved-position-sensitive (PSD) from INEL (CPS 120) and a high-temperature attachment from Rigaku. The detector was used in a semi-focusing arrangement by reflection ($\text{CuK}\alpha_1$ radiation) as described elsewhere [19].

3. Results and discussion

3.1. Structure solution

The structure was solved in space group $P6_422$. The heavy atoms were located using both direct methods and Patterson function with SIR97 [20] and SHELXS97 [21] available in the WinGX software package [22]. The remaining atoms were located from successive Fourier map analyses using SHELXL97 [23]. The last cycles of

the refinement included atomic coordinates and anisotropic displacement parameters for all atoms. The occupancy factor of the oxygen atom from the water molecule Ow4 located inside the channels was freed and refined to a value of 0.51(2), leading to the chemical formulation $\text{Cd}_3\text{In}_2(\text{C}_2\text{O}_4)_6 \cdot 9.03(4)\text{H}_2\text{O}$ for the title compound. The maximum residual electronic density peak of 2.138 e Å^{-3} could correspond to the presence of another disordered water molecule inside the voids of the structure, but was finally left out because it led to an inconsistent displacement parameter. At this stage of the study it must be noted that there is an ambiguity in the positioning of In and Cd atoms due to the one electron difference between them. According to the Cd/In ratio found from EDS and TG analysis, there are four possibilities for the repartition of the three Cd and two In atoms on the four crystallographic sites 6*f*, 3*a*, 3*c* and 3*d*. The results of the refinements for the four cases were as follows: (i) Cd in 6*f* and 3*a*, In in 3*c* and 3*d* ($R_1 = 3.78\%/wR_2 = 9.45\%/GoF = 1.135$); (ii) Cd in 6*f* and 3*c*, In in 3*a* and 3*d* ($3.60\%/9.07\%/1.095$); (iii) Cd in 6*f* and 3*d*, In in 3*a* and 3*c* ($3.74\%/9.46\%/1.136$); (iv) In in 6*f* and Cd in 3*a*, 3*c* and 3*d* ($3.62\%/9.07\%/1.097$). Although the differences between the *R* and GoF factors are small, the values for (ii) and (iv) are slightly lower. These two cases have then been analyzed according to the distances In–O and Cd–O reported in the literature for eight-fold coordinated metals, namely In–O distances in the relatively narrow range 2.19–2.38 Å [12,13] and Cd–O distances in the broader range 2.27–2.64 Å with, usually, four shorter and four longer distances [4,5,7,8,24–26]. In the selected models (ii) and (iv), the distances are in the range 2.17–2.69 Å for position 3*d*, which is in favor of a Cd atom as found in model (iv). This is also in accordance with the distorted polyhedra sometimes reported for CdO_8 [11]. Consequently, the crystal structure of $\text{Cd}_3\text{In}_2(\text{C}_2\text{O}_4)_6 \cdot 9\text{H}_2\text{O}$ will be described below according the suggested model (iv). The final atomic coordinates, together with their equivalent isotropic displacement parameters, are listed in Table 2. Selected bond distances and angles are reported in Table 3.

3.2. Description of the structure

The structure of $\text{Cd}_3\text{In}_2(\text{C}_2\text{O}_4)_6 \cdot 9\text{H}_2\text{O}$ is a three-dimensional network constituted by the assembly of MO_8 ($M = \text{Cd}, \text{In}$) polyhedra and oxalate moieties. It displays a porous framework with square cross-section channels, along **a**, **b** and **a + b**, filled by weakly bonded water molecules. The nature of the different polyhedra constitutive of the framework was determined using Haigh's criterion based upon the pattern of O–*M*–O bond angles [10]. Indeed, this criterion is convenient when trying to attribute a geometry to eight-fold metal environments. It results from this analysis that the

Table 2

Fractional atomic coordinates and equivalent isotropic atomic displacement parameters with their standard deviations for $\text{Cd}_3\text{In}_2(\text{C}_2\text{O}_4)_6 \cdot 9\text{H}_2\text{O}$ $U_{\text{eq}} = (1/2) \sum_i \sum_j U_{ij} a_i^* a_j^* \mathbf{a}_i \cdot \mathbf{a}_j$

Atom	<i>x</i>	<i>y</i>	<i>z</i>	U_{eq} (Å ²)
In	−1/2	0	0.22196(1)	0.0185(1)
Cd1	0	0	1/3	0.0183(1)
Cd2	−1/2	−1/2	1/6	0.0345(2)
Cd3	0	−1/2	1/3	0.0429(2)
O1	−0.5785(5)	−0.2481(6)	0.1881(1)	0.032(1)
O2	−0.2951(6)	0.1655(5)	0.2639(1)	0.0296(9)
O3	0.1205(5)	0.2897(5)	0.35880(9)	0.0285(8)
O4	−0.3916(5)	−0.1775(5)	0.2504(1)	0.0296(8)
O5	−0.7562(5)	−0.0661(5)	0.1885(1)	0.0306(9)
O6	−0.2052(5)	−0.1697(5)	0.2927(1)	0.033(1)
C1	−0.7048(5)	−0.2952(5)	1/6	0.022(1)
C2	−0.1928(5)	−0.3856(9)	1/2	0.023(1)
C3	−0.2782(7)	−0.1775(7)	0.3921(1)	0.023(1)
C4	−0.2261(7)	−0.3213(7)	0.3838(1)	0.023(1)
Ow1	−0.244(1)	0	1/2	0.139(6)
Ow2	1/2	1/2	0.2241(2)	0.22(1)
Ow3	−0.2111(9)	0.3072(7)	0.3718(2)	0.075(2)
Ow4	0	−1/2	0.4498(4)	0.14(1)

framework is built up from three different types of eight-fold coordination polyhedra. Indeed, the indium atom displays a bicapped trigonal prismatic (also called hendecahedral) oxygen environment represented in Fig. 1a, while the cadmium atoms display two kinds of environments: a dodecahedral geometry for Cd1 and Cd3, shown in Fig. 1b using the Hoard and Silverton formalism [9], and a distorted polyhedra for Cd2 with an undefined shape (Fig. 1c).

The assembly of these three different polyhedra leads to a structure for $\text{Cd}_3\text{In}_2(\text{C}_2\text{O}_4)_6 \cdot 9\text{H}_2\text{O}$, which can be considered as constituted of three structurally identical domains, labeled A–C in Fig. 2a. Indeed, these domains strictly possess the same arrangement, but they are rotated by 120° along the *c*-axis with respect to each other. Each domain in Fig. 2 can itself be viewed as a stack of two distinct structural parts. The first one, shown in Fig. 2b, consists of infinite chains in the (*ab*) plane that are built from edge-sharing dodecahedra with a $-\text{Cd}1\text{O}_8-\text{Cd}3\text{O}_8-$ sequence. All oxygen atoms from the Cd1 coordination environment are atoms belonging to oxalate groups. Half the oxygen atoms surrounding Cd3 also belongs to oxalate groups (two edges are shared with two Cd1O₈ dodecahedra), while the remaining four are Ow3 from water molecules. The mean Cd–O distances are 2.30 and 2.46 Å for Cd1 and Cd3, respectively. It is worth noting that the Cd3 has four short bond lengths with Ow3 and four longer ones with O3 from oxalate moieties. The second structural part of a domain (Fig. 2c) is a two-dimensional array of Cd2O₈ and InO₈ polyhedra and oxalate entities. This sheet is formed by chains of bicapped triangular prisms InO₈ linked together through bidentate oxalate groups and

Table 3

Bond distances (Å) and angles (deg) with their standard deviations for $\text{Cd}_3\text{In}_2(\text{C}_2\text{O}_4)_6 \cdot 9\text{H}_2\text{O}$. Bond distances are given according to the notation used by Hoard and Silvertown [9]

Within the Cd1O_8 polyhedra			
<i>M–A</i>		<i>M–B</i>	
$\text{Cd1–O6, O6}^{\text{i,ii,iii}}$	2.238(4)	$\text{Cd1–O3, O3}^{\text{i,ii,iii}}$	2.364(4)
a			
O3–O3^{i}	2.628(7)	O6–O6^{ii}	3.255(8)
$\text{O3}^{\text{ii}}\text{–O3}^{\text{iii}}$	2.628(7)	$\text{O6–O6}^{\text{iii}}$	3.282(8)
		$\text{O6}^{\text{i}}\text{–O6}^{\text{ii}}$	3.282(8)
		$\text{O6}^{\text{i}}\text{–O6}^{\text{iii}}$	3.255(8)
m			
O3–O6^{i}	2.679(5)	O3–O6^{ii}	2.929(5)
$\text{O3}^{\text{i}}\text{–O6}$	2.679(5)	$\text{O3–O6}^{\text{iii}}$	2.846(6)
$\text{O3}^{\text{ii}}\text{–O6}^{\text{iii}}$	2.679(5)	$\text{O3}^{\text{i}}\text{–O6}^{\text{ii}}$	2.846(6)
$\text{O3}^{\text{iii}}\text{–O6}^{\text{ii}}$	2.679(5)	$\text{O3}^{\text{i}}\text{–O6}^{\text{iii}}$	2.929(5)
		$\text{O3}^{\text{ii}}\text{–O6}$	2.929(5)
		$\text{O3}^{\text{ii}}\text{–O6}^{\text{i}}$	2.846(6)
		$\text{O3}^{\text{iii}}\text{–O6}$	2.846(6)
		$\text{O3}^{\text{iii}}\text{–O6}^{\text{i}}$	2.929(5)
g			
			2.929(5)
Within the Cd3O_8 polyhedra			
<i>M–A</i>		<i>M–B</i>	
$\text{Cd3–O3}^{\text{ii,iii,iv,v}}$	2.664(4)	$\text{Cd3–Ow3}^{\text{ii,iii,iv,v}}$	2.263 (5)
a			
$\text{O3}^{\text{ii}}\text{–O3}^{\text{iii}}$	2.628(7)	$\text{Ow3}^{\text{ii}}\text{–Ow3}^{\text{iv}}$	3.47(1)
$\text{O3}^{\text{iv}}\text{–O3}^{\text{v}}$	2.628(7)	$\text{Ow3}^{\text{ii}}\text{–Ow3}^{\text{v}}$	3.27(1)
		$\text{Ow3}^{\text{iii}}\text{–Ow3}^{\text{iv}}$	3.27(1)
		$\text{Ow3}^{\text{iii}}\text{–Ow3}^{\text{v}}$	3.47(1)
m			
$\text{O3}^{\text{ii}}\text{–Ow3}^{\text{iv}}$	3.176(7)	$\text{O3}^{\text{ii}}\text{–Ow3}^{\text{ii}}$	2.960(7)
$\text{O3}^{\text{iii}}\text{–Ow3}^{\text{v}}$	3.176(7)	$\text{O3}^{\text{ii}}\text{–Ow3}^{\text{iii}}$	2.959(6)
$\text{O3}^{\text{iv}}\text{–Ow3}^{\text{ii}}$	3.176(7)	$\text{O3}^{\text{iii}}\text{–Ow3}^{\text{ii}}$	2.959(6)
$\text{O3}^{\text{v}}\text{–Ow3}^{\text{iii}}$	3.176(7)	$\text{O3}^{\text{iii}}\text{–Ow3}^{\text{iii}}$	2.960(7)
		$\text{O3}^{\text{iv}}\text{–Ow3}^{\text{iv}}$	2.960(7)
		$\text{O3}^{\text{iv}}\text{–Ow3}^{\text{v}}$	2.959(6)
		$\text{O3}^{\text{v}}\text{–Ow3}^{\text{iv}}$	2.959(6)
		$\text{O3}^{\text{v}}\text{–Ow3}^{\text{v}}$	2.960(7)
g			
			2.960(7)
Within the InO_8 polyhedra			
<i>M–O</i>		<i>M–O</i>	
$\text{In–O1, O1}^{\text{vi}}$	2.277(4)	$\text{In–O4, O4}^{\text{vi}}$	2.396(4)
$\text{In–O2, O2}^{\text{vi}}$	2.261(4)	$\text{In–O5, O5}^{\text{vi}}$	2.345(4)
<i>O–O</i>		<i>O–O</i>	
O1–O2^{vi}	3.264(5)	O4–O1	2.742(5)
O1–O5	2.668(6)	O4–O2^{vi}	2.784(6)
$\text{O2}^{\text{vi}}\text{–O5}$	3.069(6)	O4–O2	2.673(5)
$\text{O1}^{\text{vi}}\text{–O2}$	3.264(5)	O4–O5^{vi}	2.967(6)
$\text{O1}^{\text{vi}}\text{–O5}^{\text{vi}}$	2.668(6)	$\text{O4}^{\text{vi}}\text{–O1}^{\text{vi}}$	2.742(5)
O2–O5^{vi}	3.069(6)	$\text{O4}^{\text{vi}}\text{–O2}$	2.784(6)
O1–O5^{vi}	2.784(6)	$\text{O4}^{\text{vi}}\text{–O2}^{\text{vi}}$	2.673(5)
$\text{O1}^{\text{vi}}\text{–O5}$	2.784(6)	$\text{O4}^{\text{vi}}\text{–O5}$	2.967(6)
O2–O2^{vi}	3.226(9)		
g			
Within the Cd2O_8 polyhedra			
<i>M–O</i>		<i>M–O</i>	
$\text{Cd2–Ow1}^{\text{vii,viii}}$	2.195(9)	$\text{Cd2–O1, O1}^{\text{xi,xii,xiii}}$	2.685(4)
$\text{Cd2–Ow2}^{\text{ix,x}}$	2.171(8)		
g			
Within the oxalate moieties			
$\text{C1–C2}^{\text{xiv}}$	1.519(9)	$\text{O1–C1–O1}^{\text{xiii}}$	123.6(7)
$\text{C1–O1, O1}^{\text{xiii}}$	1.246(5)	$\text{O5–C2}^{\text{xiv}}\text{–O5}^{\text{xiii}}$	126.8(7)
$\text{C2}^{\text{xiv}}\text{–O5, O5}^{\text{xiii}}$	1.254(5)	$\text{C1–C2}^{\text{xiv}}\text{–O5, O5}^{\text{xiii}}$	116.6(3)

Table 3 (Continued)

C3–C4	1.538(7)	$\text{C2}^{\text{xiv}}\text{–C1–O1, O1}^{\text{xiii}}$	118.2(3)
$\text{C3–O4}^{\text{iii}}$	1.254(6)	$\text{O4}^{\text{iii}}\text{–C3–O6}^{\text{iii}}$	126.0(5)
$\text{C3–O6}^{\text{iii}}$	1.257(6)	$\text{O2}^{\text{iii}}\text{–C4–O3}^{\text{ii}}$	126.0(5)
$\text{C4–O2}^{\text{iii}}$	1.259(6)	$\text{C3–C4–O2}^{\text{iii}}$	117.1(4)
C4–O3^{ii}	1.240(6)	$\text{C3–C4–O3}^{\text{ii}}$	116.9(5)
		$\text{C4–C3–O4}^{\text{iii}}$	116.6(5)
		$\text{C4–C3–O6}^{\text{iii}}$	117.4(5)

Symmetry codes: (i) $-x, -x+y, 2/3-z$; (ii) $-x, -y, z$; (iii) $x, x-y, 2/3-z$; (iv) $x, -1+y, z$; (v) $-x, -1-x+y, 2/3-z$; (vi) $-1-x, -y, z$; (vii) $x-y, x, -1/3+z$; (viii) $-1-x+y, -1-x, -1/3+z$; (ix) $-1+x, -1+y, z$; (x) $-1+y, -1+x, 1/3-z$; (xi) $-1-x, -1-y, z$; (xii) $y, x, 1/3-z$; (xiii) $-1-y, -1-x, 1/3-z$; (xiv) $-1+x-y, x, -1/3+z$; (xv) $-1+y, x, 1/3-z$; (xvi) $-1-x, -1-x+y, 2/3-z$.

running in the (*ab*) plane. Each chain is linked to two adjacent ones through Cd2O_8 polyhedra. Indeed, the oxalate group belonging to the chain also spans the Cd2 cadmium. The mean *M–O* bond lengths found within these polyhedra are 2.32 and 2.43 Å for In and Cd2, respectively. Similarly to Cd3, Cd2 has four short and four longer *M–O* distances (Table 3). It can be noted that Cd2 and Cd3 have greater atomic displacements parameters than Cd1 and In (Table 2). This feature can be related to the presence of water molecules in their coordination polyhedron. Finally, the whole domain is then reconstituted by linking the cadmium chains with the mixed In/Cd sheets. This is achieved by connecting half the InO_8 polyhedra within one sheet to each Cd1O_8 of the above chain through an oxalate group, as represented by dotted lines in Figs. 2b and c. The remaining half of the InO_8 polyhedra ensures the connection to the cadmium chains located under the sheet. The weakly bonded water molecule Ow4 is located on the *c* axis in tunnels of the structure (Fig. 2a).

The distances reported in Table 3 for oxalate moieties are in good agreement with the mean values of 1.55 Å, 1.24 Å, 117° and 125° for C–C, C–O bond lengths, C–C–O and O–C–O angles reported by Hahn for oxalate compounds [27]. An interesting feature of the oxalate entities is the variety of connection modes encountered in this structure. Indeed, the structural arrangement displays three kinds of connection between the oxalate groups and the metal atoms. One of the oxalate anion chelates two In atoms and a Cd2 atom (Fig. 3a). It is worth noting that Cd2 is spanned by two O atoms attached to the same C atom. Although it is not frequent, it has been reported in a few oxalates and carboxylates [28–31]. The other oxalate anion acts as a bidentate ligand towards Cd1 and In, but also as a monodentate ligand towards Cd3 (Fig. 3b).

3.3. Relationships with compounds built up from MO_8 polyhedra and oxalate groups

It is interesting to compare this structure with two other structure types reported for metal-oxalate-based

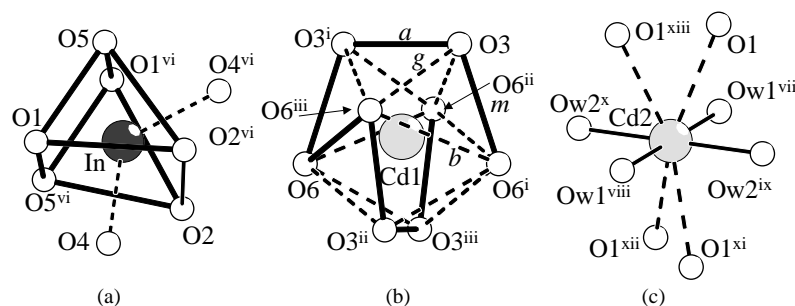


Fig. 1. The three different polyhedral shapes in the structure of $\text{Cd}_3\text{In}_2(\text{C}_2\text{O}_4)_6 \cdot 9\text{H}_2\text{O}$: (a) bicapped trigonal prism, (b) triangular dodecahedron and (c) distorted CdO_8 polyhedron. The O–O distances are indicated according to the notation used by Hoard and Silverton [9].

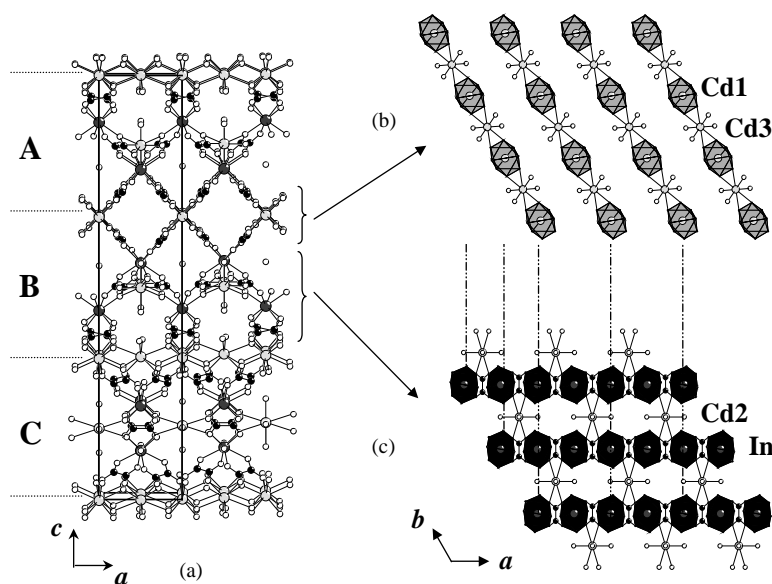


Fig. 2. (a) Projection of the $\text{Cd}_3\text{In}_2(\text{C}_2\text{O}_4)_6 \cdot 9\text{H}_2\text{O}$ structure along the b -axis showing the three identical domains A, B and C. A domain is itself constituted of (b) infinite $[-\text{Cd1O}_8-\text{Cd3O}_8-]$ chains connected to (c) sheets made of Cd2O_8 and InO_8 polyhedra.

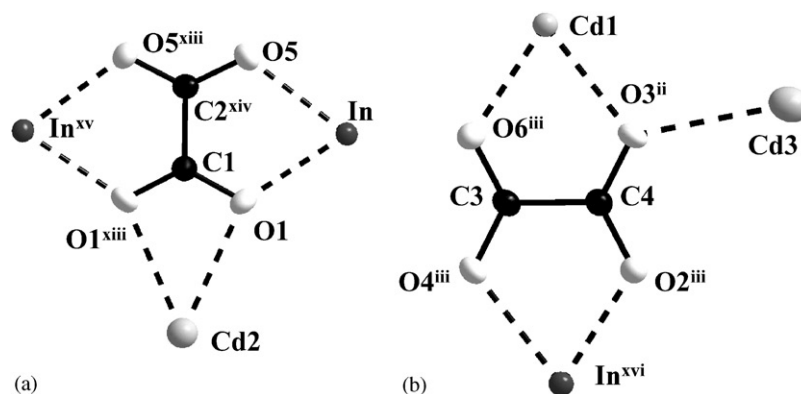


Fig. 3. Representation of the connecting modes observed for the oxalate groups. Atomic displacement ellipsoids are plotted at the 50% probability level.

compounds. Indeed, relationships can be found with the ‘tetragonal’ structural type adopted, for example, by $\text{CdZrK}_2(\text{C}_2\text{O}_4)_4 \cdot 8\text{H}_2\text{O}$ [4] as well as with the ‘hexagonal’ type displayed by $\text{CdZrNa}_2(\text{C}_2\text{O}_4)_4 \cdot 8.5\text{H}_2\text{O}$ [5]. In

the following discussion, the term ‘anionic framework’ refers to the three-dimensional framework made of MO_8 polyhedra linked together through oxalate groups only. The topology of the mixed cadmium indium structure is

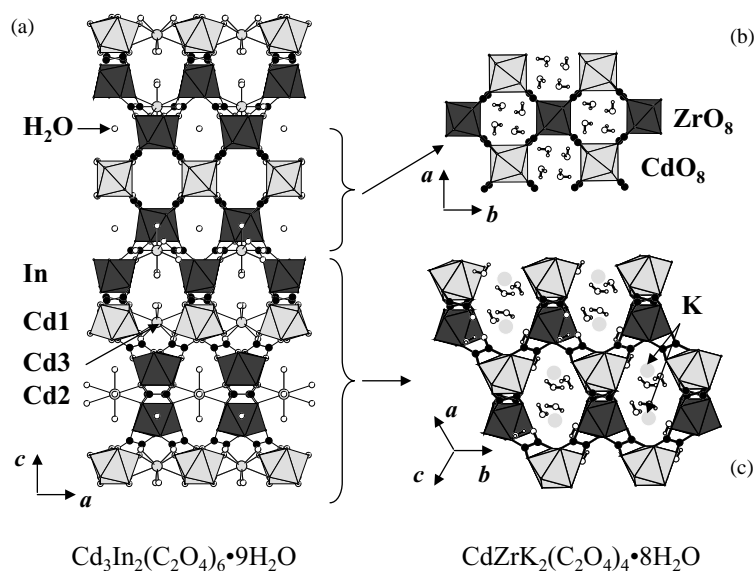


Fig. 4. Comparison between the structural arrangements of (a) $\text{Cd}_3\text{In}_2(\text{C}_2\text{O}_4)_6 \cdot 9\text{H}_2\text{O}$ viewed along b and that of $\text{CdZrK}_2(\text{C}_2\text{O}_4)_4 \cdot 8.5\text{H}_2\text{O}$ viewed along (b) the c -axis and (c) $[111]$. The polyhedron representation is used for the atoms connected through oxalate groups only.

related to that of the tetragonal type. The structure of $\text{Cd}_3\text{In}_2(\text{C}_2\text{O}_4)_6 \cdot 9\text{H}_2\text{O}$ viewed along a or b displays two kinds of tunnels (Fig. 4a) with a 'square' cross-section ($\sim 4 \text{ \AA}$, calculated from the shortest O–O contact distances not including van der Waals radii) and an 'elliptic' cross-section ($\sim 4 \times 10 \text{ \AA}$). The same kind of tunnels are also found in the tetragonal structure type but along two different directions: c for the square tunnels (Fig. 4b) and $[111]$ for the elliptic ones (Fig. 4c). While the anionic framework $[\text{CdIn}_2(\text{C}_2\text{O}_4)_6]^{4-}$ in the cadmium indium compound is constituted of dodecahedra (CdO_8) and bicapped trigonal prism (InO_8), that of the tetragonal type is only built up from dodecahedra (CdO_8 and ZrO_8). The presence of trigonal prisms in the framework of the Cd/In phase leads to a twist in the stacking sequence along the c -axis, as if the topology of the $[\text{CdIn}_2(\text{C}_2\text{O}_4)_6]^{4-}$ anionic framework was made of successive blocks, like $[\text{CdZr}(\text{C}_2\text{O}_4)_4]^{2-}$, viewed along c and along $[111]$.

The title compound can also be related to the hexagonal structure types found for example in $\text{InNa}(\text{C}_2\text{O}_4)_2 \cdot 2\text{H}_2\text{O}$, $\text{InNH}_4(\text{C}_2\text{O}_4)_2 \cdot 2\text{H}_2\text{O}$ [12], $\text{CdZr}(\text{NH}_4)_2(\text{C}_2\text{O}_4)_4 \cdot 3.9\text{H}_2\text{O}$, $\text{CdZr}(\text{C}_2\text{N}_2\text{H}_{10})(\text{C}_2\text{O}_4)_4 \cdot 4.4\text{H}_2\text{O}$ [8] or $\text{CdZrNa}_2(\text{C}_2\text{O}_4)_4 \cdot 8.5\text{H}_2\text{O}$ [5]. Indeed, the hexagonal unit-cell parameter a for all these phases roughly remains the same ($\sim 9 \text{ \AA}$), whereas the parameter c can be doubled or tripled from one compound to another. This feature can directly be related to the number of atoms constitutive of the anionic framework. For example, $\text{InNH}_4(\text{C}_2\text{O}_4)_2 \cdot 2\text{H}_2\text{O}$ has a framework built up only by one indium atom, that of $\text{CdZrNa}_2(\text{C}_2\text{O}_4)_4 \cdot 8.5\text{H}_2\text{O}$ by two different atoms (Cd and Zr) and that of $\text{Cd}_3\text{In}_2(\text{C}_2\text{O}_4)_6 \cdot 9\text{H}_2\text{O}$ by three different atoms (two In and Cd1). This feature results in a c -axis

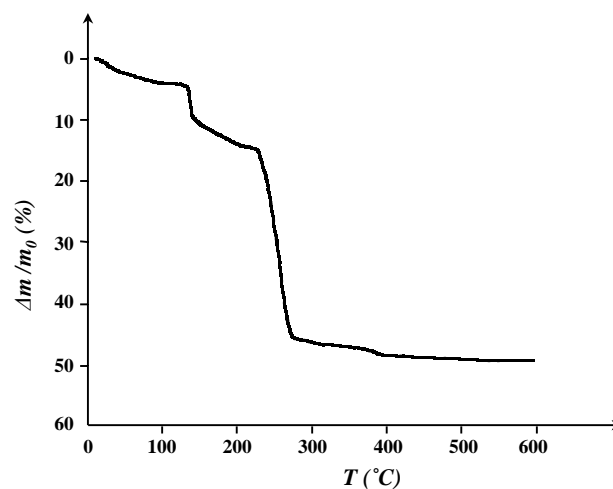


Fig. 5. TG curve for $\text{Cd}_3\text{In}_2(\text{C}_2\text{O}_4)_6 \cdot 9.5\text{H}_2\text{O}$ under flowing air (heating rate: 5°C h^{-1} between 20°C and 400°C and then 25°C h^{-1} until 600°C).

which is roughly doubled and tripled of that observed for $\text{InNH}_4(\text{C}_2\text{O}_4)_2 \cdot 2\text{H}_2\text{O}$ (11.59 \AA), namely 24.53 \AA for $\text{CdZrNa}_2(\text{C}_2\text{O}_4)_4 \cdot 8.5\text{H}_2\text{O}$ and 37.81 \AA for $\text{Cd}_3\text{In}_2(\text{C}_2\text{O}_4)_6 \cdot 9\text{H}_2\text{O}$.

3.4. Thermal behavior

The thermal decomposition of the binary compound was studied from TG measurements (Fig. 5) and TDXD (Fig. 6), from room temperature to 600°C , under airflow. The chemical formula of the precursor obtained from the TG curve is $\text{Cd}_3\text{In}_2(\text{C}_2\text{O}_4)_6 \cdot 9.5\text{H}_2\text{O}$, which is consistent with the formula derived from the crystal structure refinement. The slight excess in water is quite

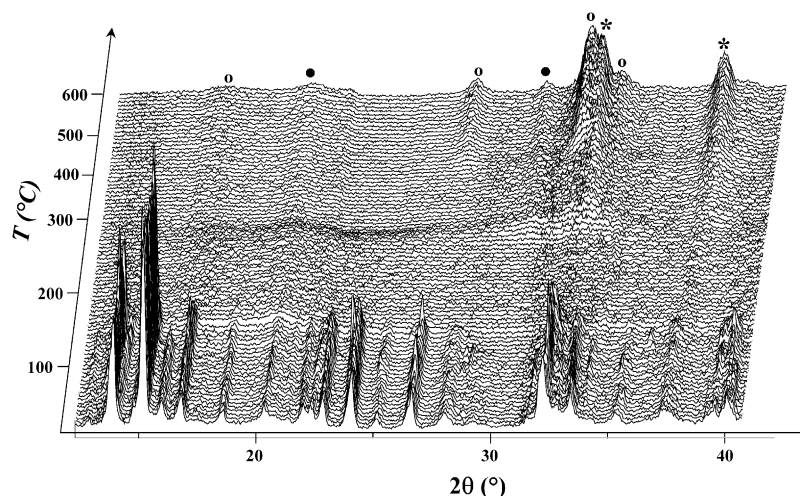


Fig. 6. TDXD plot for $\text{Cd}_3\text{In}_2(\text{C}_2\text{O}_4)_6 \cdot 9\text{H}_2\text{O}$ under flowing air (5°C h^{-1} between 20°C and 300°C and then 10° h^{-1} until 600°C , counting time: 60 min/pattern). ○, CdIn_2O_4 ; ●, In_2O_3 ; *, CdO .

frequent in these kind of porous phases. The precursor starts losing weight as soon as it is heated. A continuous weight loss of $\sim 4.1\%$ is observed until $\sim 105^\circ\text{C}$, though the dehydration is slower after 60°C . This stage can be associated with the departure of the less bonded water molecules located inside the tunnels and one structural water molecule. The plateau between 105°C and 130°C corresponds to a global composition close to $\text{Cd}_3\text{In}_2(\text{C}_2\text{O}_4)_6 \cdot 7\text{H}_2\text{O}$ (calcd. weight loss 3.6%). Until 130°C , no significant change is observed in the TDXD plot, which suggests that the overall structural arrangement is not modified by the departure of these water molecules. A second, more abrupt, weight loss of $\sim 10.1\%$ is seen between $\sim 130^\circ\text{C}$ and 215°C , which corresponds to the total dehydration of the compound with the loss of the remaining structural water molecules (calcd. 9.7%). The departure of these water molecules leads to the collapse of the structural arrangement, as confirmed by the TDXD plot with patterns corresponding to phase(s) amorphous to X-rays in the range ~ 140 – 300°C . Finally, the oxalate entities decomposition takes place between $\sim 215^\circ\text{C}$ and 300°C , as generally observed in chemically related compounds, with a weight loss of $\sim 34.5\%$ seen in the TG plot (calcd. 34.1%). The diffraction peaks of nanocrystalline cubic CdO , In_2O_3 and CdIn_2O_4 appear between 300°C and 350°C . The powder diffraction data of the final products collected ex situ with the high-resolution diffractometer confirmed the formation of the mixed cubic oxide CdIn_2O_4 (PDF2 no. 70–1680 [32]) together with cubic CdO (PDF2 no. 75–0591 [32]) and cubic In_2O_3 (PDF2 no. 88–2160 [32]), though indium oxide was the minor component. It can be anticipated that the formation of the three-oxide mixture arises from more than one phase component in the amorphous sample. One feature of the thermal decomposition should be commented, namely the reversibility of the dehydration process in the

temperature range in which the precursor structure is stable (until $\sim 140^\circ\text{C}$). An additional study has revealed that a partially dehydrated phase (weight loss 4.4% , i.e., $\sim 3\text{H}_2\text{O}$) by heating until 120°C could, subsequently, be rehydrated upon cooling at ambient temperature. It was noted that the initial water molecule content was not exactly recovered (the difference was $0.8\text{H}_2\text{O}$ with respect to the initial content). It was checked by X-ray powder diffraction that the crystal structure was preserved during the dehydration–rehydration process.

To conclude, the crystal structure of $\text{Cd}_3\text{In}_2(\text{C}_2\text{O}_4)_6 \cdot 9\text{H}_2\text{O}$ described in the present study demonstrates that new topologies can be conceived from MO_8 polyhedra linked through oxalate groups. Indeed, the present topology differs from the two distinct arrangements found in the Cd/Zr/oxalate system. Nevertheless, the description of the indium cadmium structure has clearly shown that topological relationships with the two Cd/Zr models have been pointed out. This result offers interesting possibilities for conceiving new oxalate-based materials from the assembly of MO_8 polyhedra. Finally, the thermal behavior study has shown that mixed oxides can be formed at relatively low temperature, even though CdIn_2O_4 is here mixed with the two simple oxides.

Acknowledgments

The authors thank Dr. T. Roisnel (Centre de Diffractométrie X, Université de Rennes 1) and Mr. G. Marsolier for their assistance in single-crystal and powder X-ray diffraction data collection, respectively, and they are grateful to Mr. O. Rastoix (Centre de Microscopie Electronique à Balayage et microAnalyse, Université de Rennes 1) for SEM analysis.

References

- [1] A.K. Cheetham, G. Férey, T. Loiseau, *Angew. Chem. Int. Ed.* 38 (1999) 3268–3292.
- [2] M. Eddaoudi, H. Li, T. Reineke, M. Fehr, D. Kelley, T.L. Groy, O.M. Yaghi, *Topics Catal.* 9 (1999) 105–111.
- [3] C.N.R. Rao, S. Natarajan, A. Choudhury, S. Neeraj, R. Vaidhyanathan, *Acta Crystallogr. B* 57 (2001) 1–12.
- [4] E. Jeanneau, N. Audebrand, D. Louër, *J. Mater. Chem.* 12 (2002) 2383–2389.
- [5] E. Jeanneau, N. Audebrand, M. Le Floch, B. Bureau, D. Louër, *J. Solid State Chem.* 170 (2003) 330–338.
- [6] T. Bataille, J.-P. Auffrédic, D. Louër, *Chem. Mater.* 11 (1999) 1559–1567.
- [7] E. Jeanneau, N. Audebrand, J.P. Auffrédic, D. Louër, *J. Mater. Chem.* 11 (2001) 2545–2552.
- [8] E. Jeanneau, N. Audebrand, D. Louër, *Chem. Mater.* 14 (2002) 1187–1194.
- [9] J.L. Hoard, J.V. Silverton, *Inorg. Chem.* 2 (1963) 235–243.
- [10] C.W. Haigh, *Polyhedron* 14 (1995) 2871–2878.
- [11] C.W. Haigh, *Polyhedron* 15 (1996) 605–643.
- [12] N. Bulc, L. Golič, J. Šiftar, *Acta Crystallogr. C* 39 (1983) 176–178.
- [13] N. Audebrand, S. Raite, D. Louër, *Solid State Sciences*, in press.
- [14] Nonius, Kappa CCD Program Software, Nonius BV, Delft, The Netherlands, 1998.
- [15] Z. Otwinowski, W. Minor, *Methods Enzymol.* 276 (1997) 307–326.
- [16] P. Coppens, in: F.R. Ahmed, S.R. Hall, C.P. Huber (Eds.), *Crystallographic Computing*, Munksgaard Publishers, Copenhagen, 1970, pp. 255–270.
- [17] K. Brandenburg, M. Berndt, *Diamond, Crystal Impact*, Bonn, 2001 (version 2.1e).
- [18] D. Louër, J.I. Langford, *J. Appl. Crystallogr.* 21 (1988) 430–437.
- [19] J. Plévert, J.P. Auffrédic, M. Louër, D. Louër, *J. Mater. Sci.* 24 (1989) 1913–1918.
- [20] A. Altomare, M.C. Burla, M. Camalli, G. Cascarano, C. Giacovazzo, A. Guagliardi, A.G.G. Moliterni, G. Polidori, R. Spagna, *J. Appl. Crystallogr.* 32 (1999) 115–119.
- [21] G.M. Sheldrick, *Acta Crystallogr. A* 46 (1990) 467–473.
- [22] L.J. Farrugia, *J. Appl. Crystallogr.* 32 (1999) 837–838.
- [23] G.M. Sheldrick, *Acta Crystallogr. A* 46 (1990) 467–473; G.M. Sheldrick, *SHELXL-97: Programs for Crystal Structure Refinement*, University of Göttingen, Göttingen, 1997.
- [24] A. Prasad, S. Neeraj, S. Natarajan, C.N.R. Rao, *Chem. Commun.* 14 (2001) 1251–1252.
- [25] B. Matkovic, B. Ribar, B. Zelenko, *Acta Crystallogr.* 21 (1966) 719–725.
- [26] K.H. Chung, E. Hong, Y. Do, C.H. Moon, *Chem. Commun.* 22 (1995) 2333–2334.
- [27] T. Hahn, *Z. Kristallogr.* 109 (1957) 438–466.
- [28] R. Vaidhyanathan, S. Natarajan, C.N.R. Rao, *J. Solid State Chem.* 162 (2001) 150–157.
- [29] B. Gomez-Lor, E. Gutiérrez-Puebla, M. Iglesias, M.A. Monge, C. Ruiz-Valero, N. Snejko, *Inorg. Chem.* 41 (2002) 2429–2432.
- [30] M. Hernández-Molina, P. Lorenzo-Luis, C. Ruiz-Pérez, T. López, I.R. Martín, K.M. Anderson, A.G. Orpen, E. Bocanegra, F. Lloret, M. Julve, *J. Chem. Soc. Dalton Trans.* 18 (2002) 3462–3470.
- [31] R. Vaidhyanathan, S. Natarajan, C.N.R. Rao, *Inorg. Chem.* 41 (2002) 5226–5234.
- [32] Powder Diffraction File, International Centre for Diffraction Data, Newtown Square, PA.